

Quantum Hall Effect on the Hofstadter Butterfly

Mikito Koshino and Tsuneya Ando

Department of Physics, Tokyo Institute of Technology 2-12-1 Ookayama, Meguro-ku, Tokyo 152-8551, Japan

(Dated: March 23, 2022)

Motivated by recent experimental attempts to detect the Hofstadter butterfly, we numerically calculate the Hall conductivity in a modulated two-dimensional electron system with disorder in the quantum Hall regime. We identify the critical energies where the states are extended for each of butterfly subbands, and obtain the trajectory as a function of the disorder. Remarkably, we find that, when the modulation becomes anisotropic, the critical energy branches accompanying a change of the Hall conductivity.

The problem of a Bloch electron in a magnetic field in two dimensions has long been investigated. Theoretically, the interplay of the modulation and the magnetic field gives rise to a recursive set of energy gaps as a sensitive function of the field amplitude, which is known to be the Hofstadter butterfly [1]. It is also predicted that the system exhibits the quantum Hall effect when the Fermi energy is in each single gap, where the gap-rich structure leads to the nontrivial sequence of the quantized Hall conductivities [2]. On the experimental side, many efforts have been devoted to the challenge of observing the Hofstadter butterfly mainly in lateral superlattices patterned on GaAs/AlGaAs heterostructures [3, 4, 5]. A remnant of the nonmonotonic behavior of the Hall conductivity peculiar to the Hofstadter butterfly was observed [4].

In a two-dimensional (2D) electron system without periodic potentials, it is generally believed that the weak disorder makes almost all the states localized leaving the extended states at the center of the Landau band, and the Hall conductivity jumps from one integer to another when the Fermi energy sweeps through the extended states. It is natural to expect in a periodic system that each butterfly subband exhibiting a non-zero Hall conductivity has extended states at specific energies. It is an intriguing problem how these energies move and how the nonmonotonic behavior of the Hall conductivity changes as a function of disorder strength, until the butterfly structure is eventually destroyed.

The problems of the quantum Hall effect and Anderson localization in the disordered 2D Bloch system have been studied by several authors. The evolution of the extended states has been investigated in tight-binding lattices, from the viewpoint of the disappearance of the quantum Hall effect in the weak-field limit [6, 7, 8, 9, 10, 11]. The pair annihilation of extended states with the increase in randomness was demonstrated [6] and the Hall conductivity was also calculated [9]. The nonmonotonic behavior of the Hall conductivity was demonstrated for the Hofstadter butterfly in the presence of disorder [12]. A finite-size scaling analysis was performed for a 2D system modulated by a weak periodic potential and the critical exponent was estimated at the center of the Landau level [13]. A qualitative discussion on the evolution of the extended states in the Hofstadter butterfly as a function of the disorder for several flux states was given [14, 15].

In this paper, we study the scaling property of the

Hall conductivity σ_{xy} in a weakly modulated 2D electron system, and identify the critical energies for each of butterfly subbands. We obtain the trajectory in the energy-disorder space to show how the energies move as a function of disorder. We also find that the number of critical energies sensitively depends on the *anisotropy* of the periodic potential, which is controllable in a real experiment.

Let us consider a two-dimensional system in a strong magnetic field with a square periodic potential

$$V_p(x, y) = V_x \cos \frac{2\pi}{a}x + V_y \cos \frac{2\pi}{a}y. \quad (1)$$

The band structure is characterized by the parameter $\phi = Ba^2/(h/e)$, a number of magnetic flux quanta penetrating a unit cell [1]. The disorder potential V_d is taken as the randomly distributed delta potential $\pm v_0$ with the concentration $2\pi l^2 n_i = 4$, where l is the magnetic length and n_i is the number of scatterers in a unit area [16]. The energy scale for the disorder is then given by $\Gamma = 4n_i v_0^2/(2\pi l^2)$ [17]. The magnetic field is assumed to be sufficiently strong so that V_p and Γ are smaller than the cyclotron energy $\hbar\omega_c$, and so that we can consider only the lowest Landau level. To deal with a finite system, we consider the larger unit cell $L \times L$ with $L = Ma$ (M : integer) and apply the periodic boundary condition. We calculate the Hall conductivity using the Kubo formula for zero temperature,

$$\sigma_{xy} = \frac{\hbar e^2}{iL^2} \sum_{\epsilon_\alpha < E_F} \sum_{\epsilon_\beta \neq \epsilon_\alpha} \frac{\langle \alpha | v_x | \beta \rangle \langle \beta | v_y | \alpha \rangle - \langle \alpha | v_y | \beta \rangle \langle \beta | v_x | \alpha \rangle}{(\epsilon_\alpha - \epsilon_\beta)^2}, \quad (2)$$

where ϵ_α is the energy of the eigenstate $|\alpha\rangle$, E_F the Fermi energy, and v_i the velocity operator. We take into account the mixing of the states between Landau levels $n = 0$ and 1 up to the first order of $V/(\hbar\omega_c)$ with V being V_p or V_d .

We first consider an isotropic modulation, $V_x = V_y$. The calculations are performed for two different fluxes, $\phi = 3$ and $3/2$. In both cases, the lowest Landau level splits into three subbands in the absence of the disorder, while the distributions of the Hall conductivity σ_{xy} are different as shown in Fig. 1. Specifically, σ_{xy} for three subbands becomes $(0, 1, 0)$ (in units of $-e^2/h$) in $\phi = 3$ and $(1, -1, 1)$ in $\phi = 3/2$, which satisfies the Diophantine equation [2].

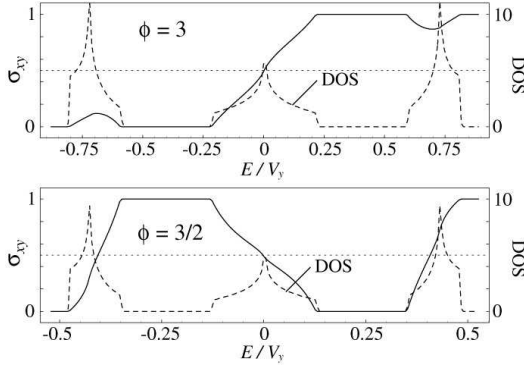


FIG. 1: Plots of the Hall conductivity σ_{xy} (in units of $-e^2/h$) for a nondisordered electron in the modulation $V_x/V_y = 1$ with $\phi = 3$ (upper) and $3/2$ (lower). Dashed lines represent the density of states in units of $1/(V_y a^2)$.

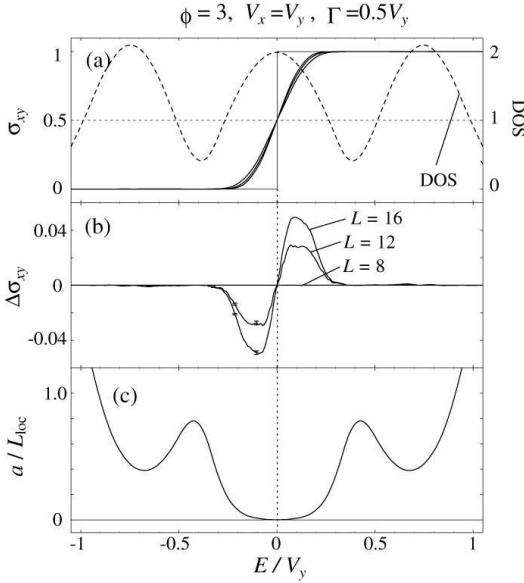


FIG. 2: (a) Hall conductivity σ_{xy} (in units of $-e^2/h$) calculated for disordered systems with $V_x/V_y = 1$, $\Gamma/V_y = 0.5$, $\phi = 3$, and $L/a = 8, 12$, and 16 . The dashed line represents the density of states in units of $1/(V_y a^2)$. (b) Relative values of σ_{xy} measured from the smallest ($L/a = 8$) sample. (c) Inverse localization length (in units of a) estimated from the Thouless number method [16]. The vertical dashed line penetrating the panels represents the critical energy.

Figures 2 and 3 show the numerical results calculated for the disordered systems with several sizes for $\phi = 3$ and $3/2$, respectively. The panel (a) shows σ_{xy} with the density of states, and (b) the difference in σ_{xy} measured from the smallest ($L/a = 8$) sample. We also show in the panel (c) the inverse localization length $1/L_{loc}$ estimated by the Thouless number method [16]. We divide the energy axis into 200 columns and every quantity is averaged over a number of different samples for each column.

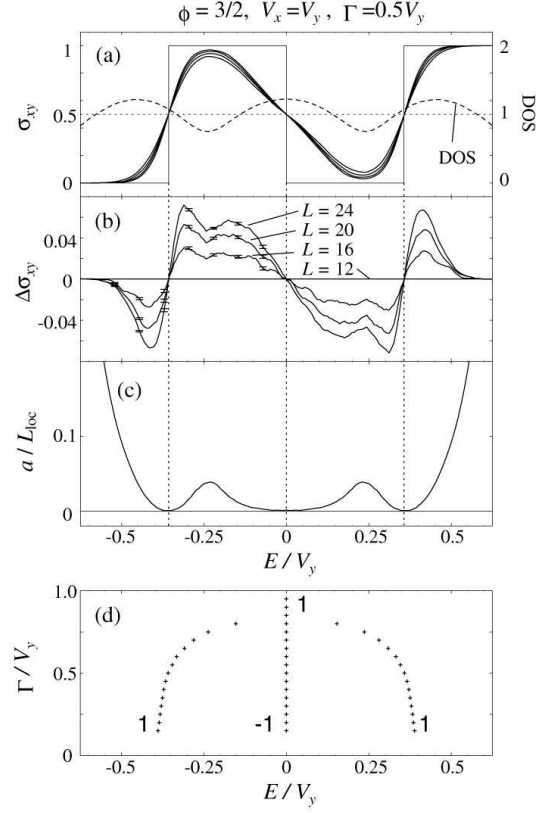


FIG. 3: Plots similar to Fig. 2, for $V_x/V_y = 1$, $\Gamma/V_y = 0.5$, and $\phi = 3/2$ with $L/a = 12, 16, 20$, and 24 . The panel (d) shows the trajectories of the critical energies as a function of Γ . Numbers represent the corresponding Hall conductivities.

We can clearly see that the subbands with zero Hall conductivity (the upper and lower subbands in $\phi = 3$) are all localized as naturally expected, and the Hall conductivity there rapidly reaches the quantized value. Each of other bands contains a critical energy where the localization length diverges ($1/L_{loc} = 0$). The Hall conductivity for these delocalized bands has fixed points at $\sigma_{xy} = 1/2$, which agree quite well with the critical energies estimated from L_{loc} . σ_{xy} off the fixed points always approaches 1 in the area $\sigma_{xy} > 1/2$ and 0 in the area $\sigma_{xy} < 1/2$, leading to the Hall plateau in an infinite system (shown as step like lines in (a)). Therefore, it is natural to define the positions of the extended states as the points of $\sigma_{xy} = 1/2$, which is exactly the method adopted in the following. The panel (d) in Fig. 3 shows the trace of the critical energies identified as the positions of $\sigma_{xy} = 1/2$ for several values of Γ . Three lines with the Hall conductivities 1, -1, and 1 become closer as the magnitude of disorder increases, and combine into one critical energy with the Hall conductivity 1.

The localization property is strongly affected by the configuration of the periodic potential itself. Here, we investigate how the above results are altered when we make the potential *anisotropic* (i.e., $V_x \neq V_y$). Figure 4

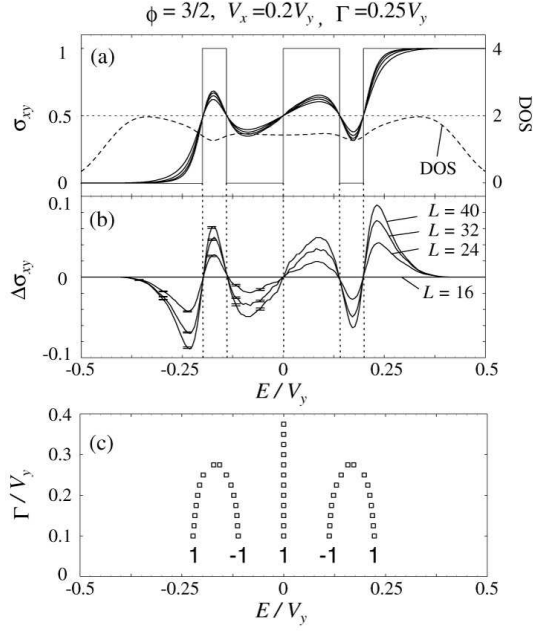


FIG. 4: (a) Hall conductivity σ_{xy} (in units of $-e^2/h$) calculated for disordered anisotropic systems with $V_x/V_y = 0.2$, $\Gamma/V_y = 0.25$, $\phi = 3/2$ and $L/a = 16, 24, 32, 40$. The dashed line represents the density of states in units of $1/(V_y a^2)$. (b) Relative values of σ_{xy} measured from the smallest ($L/a = 16$) sample. (c) Trajectories of the critical energies as a function of Γ . Numbers represent the corresponding Hall conductivities

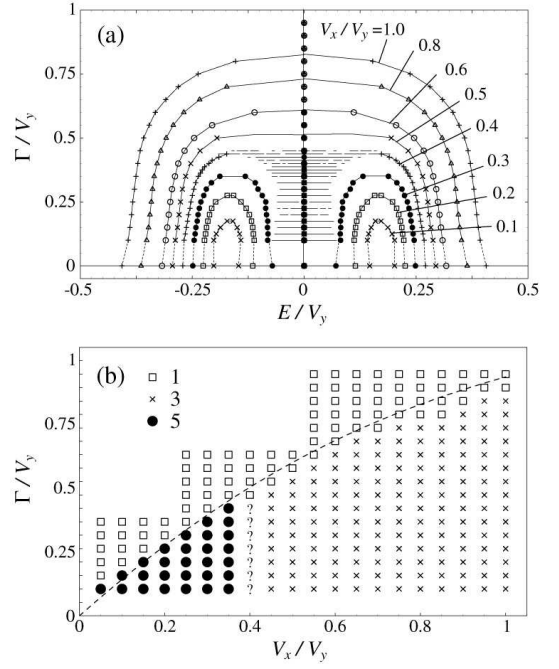


FIG. 6: (a) Traces of the critical energies for several values of V_x/V_y . For $V_x/V_y = 0.4$, we present the energy regions where the error bar of the Hall conductivity reaches $\sigma_{xy} = 1/2$. (b) Phase diagram showing the number of critical energies in the disorder (Γ/V_y)-anisotropy (V_x/V_y) space. ‘?’ indicates indeterminate. The dashed line shows $4E_G/V_y$ with E_G being the subband gap in the ideal system without disorder.

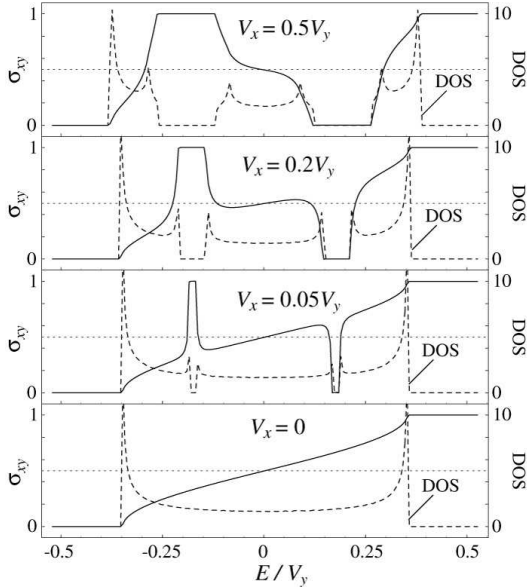


FIG. 5: Plots of the Hall conductivity σ_{xy} (in units of $-e^2/h$) for a nondisordered electron in anisotropic systems with $V_x/V_y = 0.5, 0.2, 0.05$ and 0 and $\phi = 3/2$. The dashed line represents the density of states in units of $1/(V_y a^2)$.

shows the Hall conductivity calculated for the disordered system with $V_x/V_y = 0.2$ and $\phi = 3/2$. Remarkably, we found *five* fixed points at $\sigma_{xy} = 1/2$, and they likely lead to the critical energies with the Hall conductivities 1, -1, 1, -1, and 1 in an infinite system, shown as a zig-zag line in (a). We also calculated the Thouless number, but failed to estimate the localization length around the extended region, since we cannot resolve the exponent of the size dependence of the Thouless number. However, the robust fixed points and the monotonic behavior with L in the Hall conductivity strongly suggests the existence of the critical energies at those points. The trajectories of the fixed points for several values of Γ are shown in Fig. 4(c). At a certain point, the upper and lower pairs annihilate and the center is left, which is topologically different from the isotropic case.

The origin of the five critical energies can be explained as follows. Figure 5 shows the Hall conductivity $\sigma_{xy}(E)$ for clean systems with the fixed flux $\phi = 3/2$ and various ratios of V_x/V_y . The gaps between subbands rapidly shrink as V_x/V_y goes apart from 1 and disappear at $V_x = 0$ (1D modulation), where $\sigma_{xy}(E)$ behaves just monotonically from 0 to 1. When a very small V_x is present, we see that $\sigma_{xy}(E)$ is deviated from that in $V_x = 0$ only around the subband gaps ($E - E_{\text{gap}} \lesssim V_x$). There the perturbative V_x mixes the states in $V_x = 0$ to

produce positive and negative Hall currents so that the Hall conductivity is quantized in the gap. If a small but finite disorder is introduced into this system, the critical energies with opposite Hall conductivities should exist correspondingly on each side of the gap, as long as Γ is smaller than the gap width and the Hall plateau survives. The electron-hole symmetry requires another critical energy right at the Landau band center. When V_x is switched off, the critical energy pairs at the gaps annihilate and the central one is left.

We show the corresponding plots for various values of V_x/V_y in Fig. 6(a), to explain how the isotropic (three critical energies) and anisotropic cases (five energies) are connected. We see that the center branch in the isotropic case splits into three branches at $V_x/V_y \approx 0.4$. The points at $\Gamma = 0$ show the energies of $\sigma_{xy} = 1/2$ in clean systems. The critical energies should converge to these points in the limit $\Gamma \rightarrow 0$, as long as $\sigma_{xy} = 1/2$ is the critical point for the disordered systems with a finite size. The number of such points changes from 3 to 5 at $V_x/V_y = (V_x/V_y)_0 \approx 0.36$, which defines the turning point in the evolution of the critical energy. The results (although not included in Fig. 6(a)) show that, for $V_x/V_y = 0.35 < (V_x/V_y)_0$, there are five critical energies when Γ is sufficiently small, and for $V_x/V_y = 0.45$, there are only three critical energies. In the case $V_x/V_y = 0.4$, however, it is difficult to resolve the critical energies around $E = 0$, partly because of the numerical accuracy of the calculated σ_{xy} . Therefore, we can present only the energy regions where the error bar of the Hall conductivity reaches $\sigma_{xy} = 1/2$.

We give the phase diagram in Fig. 6(b), showing the number of critical energies in the disorder (Γ/V_y)-

anisotropy (V_x/V_y) space. The newly found five-energy phase occupies a considerable area in the region of high anisotropy and low disorder. The dashed line shows $4E_G/V_y$ as a function of V_x/V_y , where E_G is the subband gap in the ideal system without disorder. The critical disorder where the number of critical energies changes from five to one or three to one roughly follows the curve as might be expected.

While we concentrated on the flux $\phi = 3/2$ here, it is expected that, in other fluxes, the butterfly gaps similarly shrink as the modulation goes to 1D and the pair annihilation of the extended states occurs at the butterfly gaps. We also assume that such a behavior does not basically change in higher Landau levels. We expect that controlling the QHE by the anisotropy proposed here is sufficiently promising for a real experiment, if a modulation is given by the external gate electrodes as in the recent experiment [4]. The existence of the fixed point at $\sigma_{xy} = 1/2$ is compatible with the two-parameter scaling theory [18], and investigating the $(\sigma_{xy}, \sigma_{xx})$ scaling in the periodic system is an important future work.

This work has been supported in part by a 21st Century COE Program at Tokyo Tech “Nanometer-Scale Quantum Physics”, a Grant-in-Aid for COE (12CE2004 “Control of Electrons by Quantum Dot Structures and Its Application to Advanced Electronics”), and Scientific Research from the Ministry of Education, Culture, Sports, and Technology, Japan. Numerical calculations were performed in part using the facilities of the Supercomputer Center, Institute for Solid State Physics, University of Tokyo.

-
- [1] D. R. Hofstadter: Phys. Rev. B **14** (1976) 2239.
 - [2] D. J. Thouless, M. Kohmoto, M. P. Nightingale, and M. den Nijs: Phys. Rev. Lett. **49** (1982) 405.
 - [3] T. Schlösser, K. Ensslin, J. P. Kotthaus, and M. Holland: Europhys. Lett. **33** (1996) 683.
 - [4] C. Albrecht, J. H. Smet, K. von Klitzing, D. Weiss, V. Umansky, and H. Schweizer: Phys. Rev. Lett. **86** (2001) 147.
 - [5] M. C. Geisler, J. H. Smet, V. Umansky, K. von Klitzing, B. Naundorf, R. Ketzmerick and H. Schweizer: Phys. Rev. Lett. **92** (2004) 256801.
 - [6] T. Ando: Phys. Rev. B **40** (1989) 5325.
 - [7] D. Z. Liu, X. C. Xie, and Q. Niu: Phys. Rev. Lett. **76** (1996) 975.
 - [8] K. Yang and R. N. Bhatt: Phys. Rev. Lett. **76** (1996) 1316.
 - [9] D. N. Sheng and Z. Y. Weng: Phys. Rev. Lett. **78** (1997) 318.
 - [10] Y. Hatsugai, K. Ishibashi, and Y. Morita: Phys. Rev. Lett. **83** (1999) 2246.
 - [11] D. N. Sheng, Z. Y. Weng, and X. G. Wen: Phys. Rev. B **64** (2001) 165317.
 - [12] H. Aoki: Surf. Sci. **263** (1992) 137.
 - [13] B. Huckestein: Phys. Rev. Lett. **72** (1994) 1080.
 - [14] Y. Tan: J. Phys. Condens. Matter **6** (1994) 7941; Phys. Rev. B **49** (1994) 1827.
 - [15] K. Yang and R. N. Bhatt: Phys. Rev. B **59** (1999) 8144.
 - [16] T. Ando: J. Phys. Soc. Jpn. **52** (1983) 1740.
 - [17] T. Ando and Y. Uemura: J. Phys. Soc. Jpn. **36** (1974) 959.
 - [18] A. M. M. Pruisken: *The Quantum Hall Effect*, eds. R. E. Prange and S. M. Girvin (Springer-Verlag, Berlin, 1990).